

## CONTACT INTERACTIONS AT FUTURE CIRCULAR COLLIDER BASED MUON–PROTON COLLIDERS\*

GURAL AYDIN

Department of Physics, Hatay Mustafa Kemal University, Hatay, 31060, Türkiye

YUSUF OGUZHAN GÜNAYDIN, MEHMET TÜRKER TARAKCIOGLU

Department of Physics, Kahramanmaraş Sütçü Imam University  
Kahramanmaraş, 46100, Türkiye

MEHMET SAHIN

Department of Computer Engineering, Usak University, Usak, 64000, Türkiye

SALEH SULTANSOY

Material Science and Nanotechnology Engineering  
TOBB Economics and Technology University  
Ankara, 06560, Türkiye  
and  
ANAS, Institute of Physics, Baku, Azerbaijan*Received 2 November 2022, accepted 3 December 2022,  
published online 19 December 2022*

Recently proposed Future Circular Collider-based muon–proton colliders will allow for investigating lepton–hadron interactions at the highest center-of-mass energy. In this study, we investigate the potential of these colliders for a four-fermion contact interactions search. Regarding the constructive and destructive interferences of contact interactions, we estimated discovery, observation, and exclusion limits on the compositeness scale for the left–left, right–right, left–right, and right–left helicity structures. In this regard, we obtained compositeness scales for the left–left helicity structure at  $\sqrt{s} = 63.2$  TeV FCC-based  $\mu p$  collider with the  $100 \text{ fb}^{-1}$  integrated luminosity as  $225.7 \pm 1.9\%$  TeV (discovery),  $269.0 \pm 2.0\%$  TeV (observation), and  $311.3 \pm 2.1\%$  TeV (exclusion). This study’s findings show that the FCC-based  $\mu p$  colliders have great potential for investigating four-fermion contact interactions.

DOI:10.5506/APhysPolB.53.11-A3

---

\* Funded by SCOAP<sup>3</sup> under Creative Commons License, CC-BY 4.0.

## 1. Introduction

The Standard Model (SM) is a theory that remarkably describes elementary particles and their strong, weak, and electromagnetic interactions. It also shows a good agreement with the experimental results on High-Energy Physics. Thus, the Standard Model gives answers to many questions about our universe. However, there are some questions that SM cannot answer. For example, why quarks and leptons repeat in families, why the Standard Model has so many parameters, how neutrinos gain their masses, and so on. To answer these questions, new theories beyond Standard Model have emerged. Among these theories, Composite Models [1–17] can respond to the best pattern to reduce the Standard Model’s parameter redundancy.

If SM fermions have a composite structure, they may consist of more fundamental particles called preons. The new physics scale on which the preons will emerge is called the compositeness scale ( $\Lambda$ ). Suppose the particle colliders’ subprocess energy is greater than the compositeness scale of fermions. In that case, research on compositeness can be done directly at particle colliders. On the other hand, research on compositeness can be performed indirectly through contact interactions (CI) if the colliders’ subprocess energy is smaller than the compositeness scale. In the literature, there are some studies on contact interactions [8, 18–27].

Contact interaction investigations were performed at electron–positron [28–32], electron–proton [33, 34], and hadron colliders [35–53] experiments. If SM leptons and quarks are composite structures,  $llqq$ -type four-fermion contact interactions occur. Here,  $l$  and  $q$  represent electron/muon and quarks, respectively. Using  $36 \text{ fb}^{-1}$  data set at  $\sqrt{s} = 13 \text{ TeV}$ , the ATLAS Collaboration puts exclusion limits on the  $llqq$ -type contact interaction scale in the  $qq \rightarrow ll$  process [54]. Contact interaction scales of the  $llqq$ -type for constructive (destructive) interference are excluded as  $\Lambda = 35$  (28) TeV and below for the right–right helicity structure,  $\Lambda = 40$  (25) TeV and below for the left–left helicity structure. The ATLAS Collaboration also excluded the  $llqq$ -type contact interaction scales  $\Lambda = 36$  (28) TeV and below for the left–right helicity structure with constructive (destructive) interference. Ditto, the CMS Collaboration puts exclusion limits on the compositeness scale as 20 TeV and 32 TeV for left–left destructive and right–right constructive cases, respectively [53].

In this paper, we investigated contact interactions at Future Circular Collider (FCC)-based muon–proton colliders. In Section 2, we give the main parameters of the FCC-based muon–proton colliders. The following section presents the Lagrangian of the contact interactions. Section 4 includes transverse momentum and pseudo-rapidity distributions that determine applied cuts in our calculations. Discovery, observation, and exclusion limit results for the compositeness scale are presented in Section 5. Our conclusion is given in the last section.

## 2. The FCC-based muon–proton colliders

The Future Circular Collider, built after the Large Hadron Collider has completed its runtime, is considered an energy-frontier machine by the high-energy physics community. Besides proton–proton collisions, electron–proton and electron–positron collision experiments are also envisaged in the FCC [55–58]. Furthermore, new solutions to the technical problems faced by muon colliders have attracted the attention of physicists to the muon–proton colliders again [59–69]. Some advantages of muon–proton colliders over other colliders can be mentioned as the reason for this orientation. First, the synchrotron radiation problem, which is encountered at very high beam energies in electron–proton colliders, is eliminated in muon–proton colliders because the muon has a heavy mass relative to the electron. Therefore, at the multi-TeV center-of-mass energy level, muon–proton colliders can be advantageous for producing new TeV-scale particles in the mass shell. Moreover, muon–proton colliders may have a lower QCD background than proton–proton colliders in the BSM studies [70]. Thus, contact interactions can be investigated more precisely at the multi-TeV scale in muon–proton colliders. Construction of the muon collider (or dedicated  $\mu$ -ring) tangential to FCC, as proposed in [71], will allow handling the highest center-of-mass energy lepton–hadron collider.

Table 1 presents the main parameters of the FCC-based muon–proton colliders for four different muon beam energies. In the FCC, colliding proton beam energy will be 50 TeV.

Table 1. Basic parameters of the FCC-based  $\mu p$  colliders [72].

Collider name	$E_\mu$ [TeV]	$\sqrt{s}$ [TeV]	$\mathcal{L}_{\text{int}}$ [ $\text{fb}^{-1}/\text{year}$ ]
$\mu 750 \otimes \text{FCC}$	0.75	12.2	5
$\mu 1500 \otimes \text{FCC}$	1.50	17.3	5
$\mu 3000 \otimes \text{FCC}$	3.00	24.5	5
$\mu 20000 \otimes \text{FCC}$	20.0	63.2	10

FCC-based  $\mu p$  collider has been expected to run for ten years. At the end of this 10-year run time, the  $\mu 750 \otimes \text{FCC}$ ,  $\mu 1500 \otimes \text{FCC}$ , and  $\mu 3000 \otimes \text{FCC}$  colliders will reach an integrated luminosity of  $50 \text{ fb}^{-1}$ , and the  $\mu 20000 \otimes \text{FCC}$  collider the luminosity of  $100 \text{ fb}^{-1}$ .

Recently, the physics potential of the FCC-based  $\mu p$  colliders has been investigated in many papers [70, 73–78].

### 3. Contact interaction Lagrangian

If fermions have a substructure, they should have a new type of interaction. Investigating these interactions depends on the center-of-mass energy of the colliders and the compositeness scale. If the compositeness scale is much greater than the center-of-mass energy of the collider, the best method to investigate these phenomena would be through four-fermion contact interactions. These interactions' most general flavor-diagonal chirally invariant Lagrangian [8, 18, 27] is described as

$$\mathcal{L}_{\text{CI}} = \frac{g_{\text{contact}}^2}{2\Lambda^2} \sum_{i,j} \eta_{ab}^{ij} (\bar{\psi}_a^i \gamma_\mu \psi_a^i) (\bar{\psi}_b^j \gamma^\mu \psi_b^j), \quad (1)$$

where  $a, b = \text{L or R}$  (for left- or right-handed chirality),  $g_{\text{contact}}^2$  is coupling constant ( $g_{\text{contact}}^2 = 4\pi$ ),  $\Lambda$  is compositeness scale, all  $\eta_{ab}^{ij}$  are chirality coefficients,  $\psi_a^i$ ,  $\bar{\psi}_a^i$ ,  $\psi_b^j$ , and  $\bar{\psi}_b^j$  are fermion spinors,  $i, j$  represent the indices of fermion species.

In this investigation, we regard four-fermion interactions ( $\mu p \rightarrow \mu + j + X$ ) whose cross section is described by  $\sigma_{\text{tot}} = \sigma_{\text{SM}} - \eta_{ij} \frac{F_I}{\Lambda^2} + \frac{F_C}{\Lambda^4}$  [43]. The first term in this equation shows the SM interactions, the second term relates to interference of the SM and four-fermion interactions, and the third term involves the contribution from pure contact interactions as a new physics (NP) only. Here, the parameters  $F_I$  and  $F_C$  are functions of the cross section not dependent on  $\Lambda$ . As the compositeness scale value rises, the term standing for the interference of contact interactions with the SM comes dominant. Then, the leading term in this research is the term denoting four-fermion contact interactions with the SM.

We first implemented this Lagrangian into the CalcHEP [79] simulation software via LanHEP [80, 81]. Then, in numerical calculations, we used the following notations:

$$A = A_{\text{LL}}^\pm \quad \text{for} \quad \left( \eta_{\text{LL}}^{ij}, \eta_{\text{RR}}^{ij}, \eta_{\text{LR}}^{ij}, \eta_{\text{RL}}^{ij} \right) = (\pm 1, 0, 0, 0), \quad (2)$$

$$A = A_{\text{RR}}^\pm \quad \text{for} \quad \left( \eta_{\text{LL}}^{ij}, \eta_{\text{RR}}^{ij}, \eta_{\text{LR}}^{ij}, \eta_{\text{RL}}^{ij} \right) = (0, \pm 1, 0, 0), \quad (3)$$

$$A = A_{\text{LR}}^\pm \quad \text{for} \quad \left( \eta_{\text{LL}}^{ij}, \eta_{\text{RR}}^{ij}, \eta_{\text{LR}}^{ij}, \eta_{\text{RL}}^{ij} \right) = (0, 0, \pm 1, 0), \quad (4)$$

$$A = A_{\text{RL}}^\pm \quad \text{for} \quad \left( \eta_{\text{LL}}^{ij}, \eta_{\text{RR}}^{ij}, \eta_{\text{LR}}^{ij}, \eta_{\text{RL}}^{ij} \right) = (0, 0, 0, \pm 1). \quad (5)$$

### 4. Transverse momentum and pseudorapidity distributions

In this study, we investigated four-fermion contact interactions at muon-proton colliders with different center-of-mass energies. We used CalcHEP simulation software in our calculations. We chose  $\mu + p \rightarrow \mu + j + X$

as a signal and as a background process. The difference between signal and background is that background does not have contact interaction vertices. Here,  $j$  denotes  $u, \bar{u}, d, \bar{d}, c, \bar{c}, s, \bar{s}, b$ , and  $\bar{b}$ .

Since the detection efficiency of jets with  $P_T$  above 20 GeV is almost 100%, any uncertainty originating from the selection of jets [46] will not be affected in our calculations with the cuts we applied. The muon beam decays in the collider ring that creates an addition to the background, which is called the beam-induced-background (BIB). According to references [82–84], BIB does not affect muon collider physics performance by some regulation of detectors. Furthermore, the LHeC Collaboration reported systematic uncertainties originated from  $\alpha_s$  and PDF are smaller than statistical uncertainties in the latest publication [85]. So, we neglected systematic errors in our calculations due to statistical uncertainties domination over the systematics.

For the quark distribution functions, we selected the CT10 [86], and for detector acceptance, we put  $P_{T_{\text{jet},\mu}} > 25$  GeV cuts on the transverse momentum of the muon and jet. In order to show the difference in the signal from the background, we obtained the transverse momentum and pseudorapidity plots by considering the CI+SM interactions as the signal process and only the SM interactions for the background.

Among these distribution plots, we have presented the transverse momentum and pseudorapidity distributions for the collider with 63.2 TeV center-of-mass energy, one of the four collider options, considering con-

$$\mu 20000 \otimes \text{FCC}, \sqrt{s} = 63.2 \text{ TeV}$$

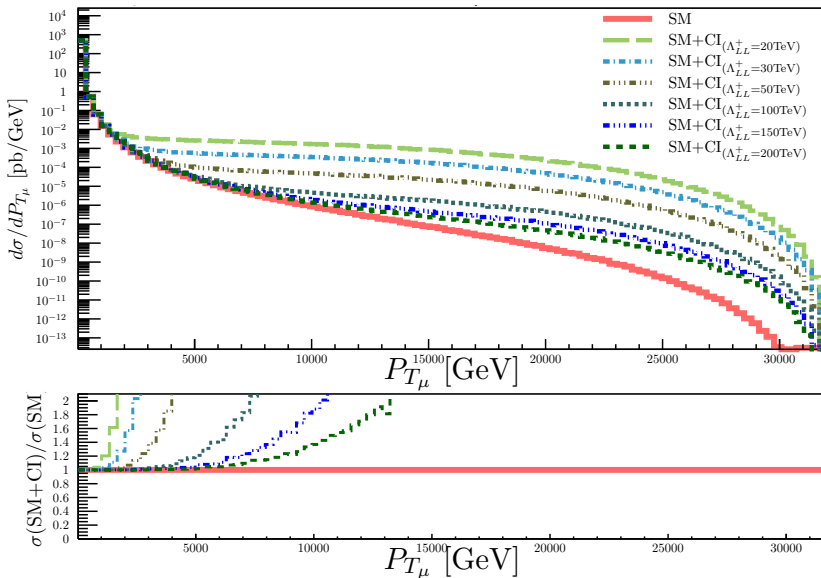


Fig. 1. Transverse momentum distribution for the final-state muon at the  $\mu 20000 \otimes \text{FCC}$  collider option with  $A_{LL}^+$ .

structive LL and destructive LL interferences as an example. As seen in Fig. 1, the point at which the  $\sigma_{(\text{CI}+\text{SM})}$  distribution begins to separate clearly from the  $\sigma_{(\text{SM})}$  distribution is 12 000 GeV. Thus, we set the cut limit  $P_{T_\mu} > 12\,000$  GeV in constructive interference for the transverse momentum of the final-state muon. Since the transverse momentum distribution function of the final-state jet also behaves exactly like the muon, we set the same cut limit for the jet.

Figure 2 shows the pseudorapidity distribution in the constructive interference for the final-state jet. According to this graph, we determined the cut on pseudorapidity as  $-4.5 < \eta_{\text{jet}} < 2$  intervals via checking the region where the CI+SM and SM distributions differ from each other. Since the CI+SM and SM pseudorapidity distributions of the final state muon show the same pattern, we chose the range of  $-2.5 < \eta_\mu < 2.5$  for the pseudorapidity cut limit.

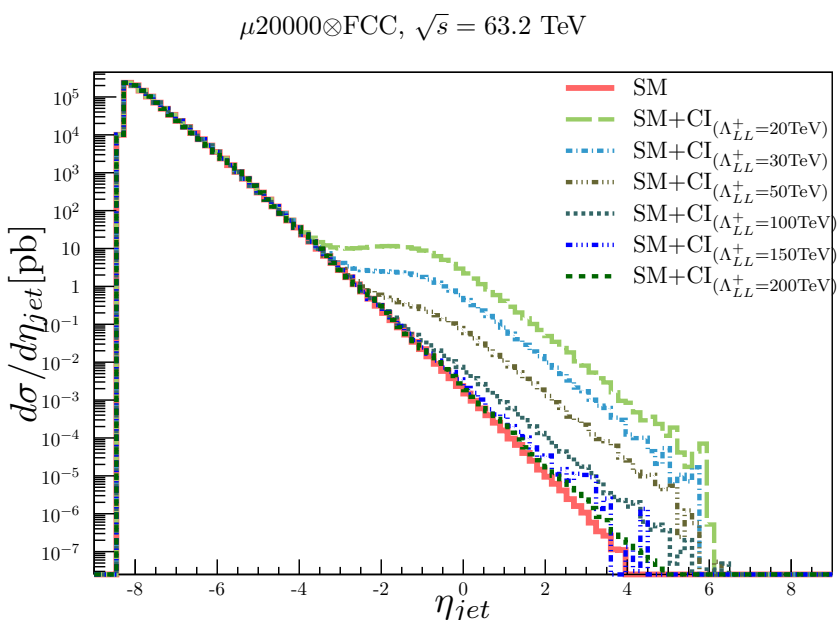


Fig. 2. Pseudorapidity distribution for the jet final state at the  $\mu 20000 \otimes \text{FCC}$  collider option with  $\Lambda_{LL}^+$ .

Using Figs. 3 and 4, for destructive interferences, we similarly set cut limits as  $P_{T_\mu} > 16\,000$  GeV,  $P_{T_{\text{jet}}} > 16\,000$  GeV,  $-5 < \eta_{\text{jet}} < 2$ , and  $-2.5 < \eta_\mu < 2.5$ . Likewise, we checked the transverse momentum and pseudorapidity distributions for the rest of the chiralities with constructive and destructive interferences. Similar analyses have been performed for each collider option and specified cut limits are listed in Table 2.

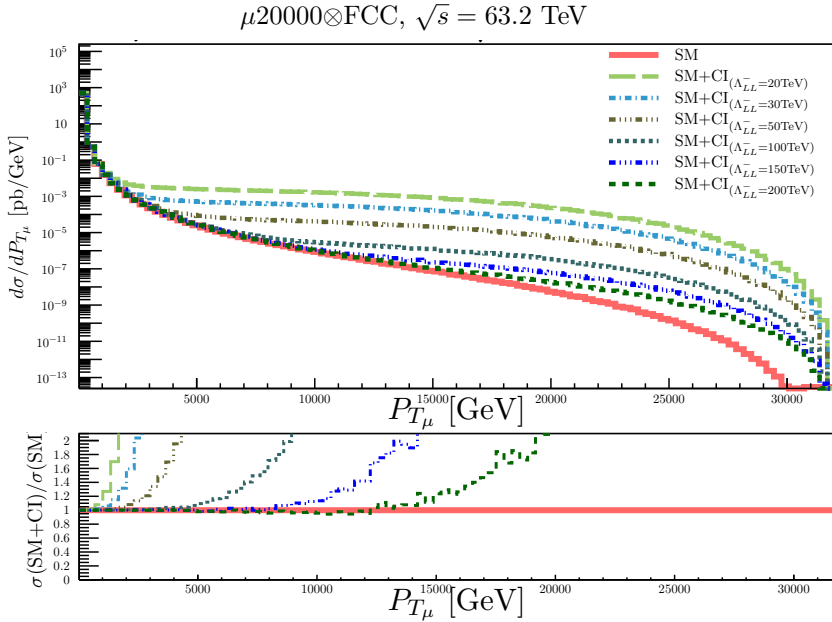


Fig. 3. Transverse momentum distribution for the final-state muon at the  $\mu 20000 \otimes \text{FCC}$  collider option with  $\Lambda_{LL}^-$ .

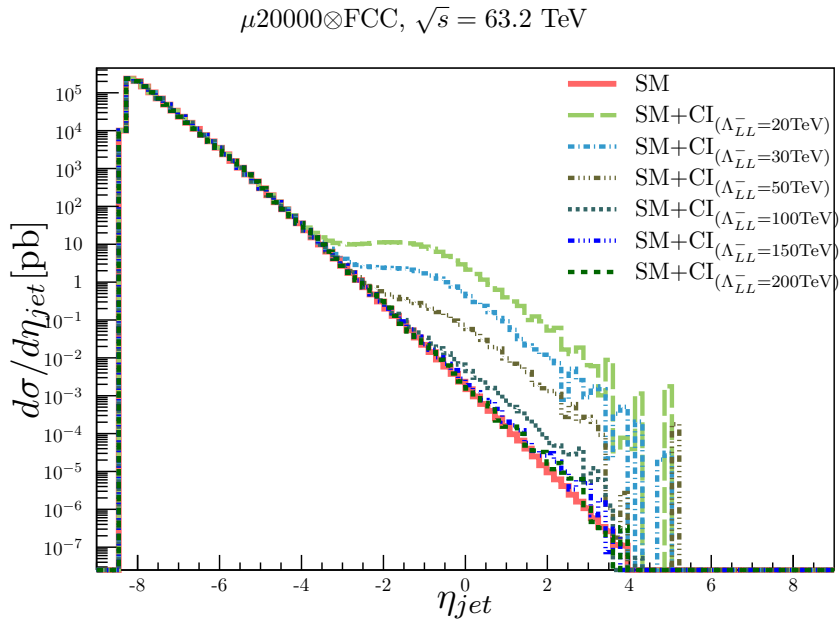


Fig. 4. Pseudorapidity distribution for the jet final state at the  $\mu 20000 \otimes \text{FCC}$  collider option with  $\Lambda_{LL}^-$ .

Table 2. Applied cut sets according to distribution plots for each collider option.

$A$	$\mu 750 \otimes \text{FCC}$ ( $\sqrt{s} = 12.2 \text{ TeV}$ )		$\mu 1500 \otimes \text{FCC}$ ( $\sqrt{s} = 17.3 \text{ TeV}$ )	
	$P_{T_{\text{jet},\mu}} [\text{GeV}]$	$\eta_{\text{jet}}$	$P_{T_{\text{jet},\mu}} [\text{GeV}]$	$\eta_{\text{jet}}$
$A_{\text{LL}}^+$	$> 2000$	$-4.5 < \eta < 1$	$> 3500$	$-4.5 < \eta < 1$
$A_{\text{LL}}^-$	$> 4000$	$-4.5 < \eta < 0.5$	$> 5500$	$-4.5 < \eta < 1$
$A_{\text{RR}}^+$	$> 2000$	$-4.5 < \eta < 1$	$> 3500$	$-4.5 < \eta < 1$
$A_{\text{RR}}^-$	$> 4000$	$-4.0 < \eta < 1$	$> 5500$	$-4.0 < \eta < 1$
$A_{\text{LR}}^+$	$> 1500$	$-4.5 < \eta < 1$	$> 2500$	$-5.0 < \eta < 1$
$A_{\text{LR}}^-$	$> 3000$	$-4.0 < \eta < 1$	$> 4000$	$-4.0 < \eta < 1$
$A_{\text{RL}}^+$	$> 1750$	$-4.5 < \eta < 1$	$> 3000$	$-4.5 < \eta < 1$
$A_{\text{RL}}^-$	$> 3000$	$-4.5 < \eta < 1$	$> 4000$	$-4.5 < \eta < 1$
$A$	$\mu 3000 \otimes \text{FCC}$ ( $\sqrt{s} = 24.5 \text{ TeV}$ )		$\mu 20000 \otimes \text{FCC}$ ( $\sqrt{s} = 63.2 \text{ TeV}$ )	
	$P_{T_{\text{jet},\mu}} [\text{GeV}]$	$\eta_{\text{jet}}$	$P_{T_{\text{jet},\mu}} [\text{GeV}]$	$\eta_{\text{jet}}$
$A_{\text{LL}}^+$	$> 4000$	$-4.5 < \eta < 1$	$> 12000$	$-4.5 < \eta < 2$
$A_{\text{LL}}^-$	$> 6000$	$-4.5 < \eta < 1$	$> 16000$	$-5.0 < \eta < 2$
$A_{\text{RR}}^+$	$> 3500$	$-4.5 < \eta < 1$	$> 11000$	$-5.0 < \eta < 2$
$A_{\text{RR}}^-$	$> 6000$	$-4.0 < \eta < 1$	$> 16000$	$-4.5 < \eta < 1$
$A_{\text{LR}}^+$	$> 2500$	$-5.0 < \eta < 1$	$> 8000$	$-5.0 < \eta < 2$
$A_{\text{LR}}^-$	$> 3500$	$-4.5 < \eta < 1$	$> 13000$	$-4.5 < \eta < 1$
$A_{\text{RL}}^+$	$> 3000$	$-4.5 < \eta < 1$	$> 10000$	$-5.0 < \eta < 1$
$A_{\text{RL}}^-$	$> 3500$	$-4.5 < \eta < 1$	$> 12000$	$-4.5 < \eta < 1$

To show applied cuts' effects on the number of events on both the CI+SM (signal) and the SM (background), we included the cut-flow table for the  $\mu 750 \otimes \text{FCC}$  collider option as an example. Table 3 illustrates the impact of cuts from Table 2 on the number of events for the  $\mu 750 \otimes \text{FCC}$  collider option. It is apparent from Table 3 that after applying all cuts, the signal events become more distinguishable than the background events.

Table 3. Cut-flow table for  $\sqrt{s} = 12.2$  TeV option with  $-2.5 < \eta_\mu < 2.5$ .

Cuts	Number of events					
	SM			CI+SM		
	No-Cuts	$\eta_{\text{jet},\mu}$	$P_{T_{\text{jet},\mu}}$	No-Cuts	$\eta_{\text{jet},\mu}$	$P_{T_{\text{jet},\mu}}$
LL+	$7.52 \times 10^8$	6215	467	$7.52 \times 10^8$	7685	1106
LL-	$7.52 \times 10^8$	6215	4	$7.52 \times 10^8$	5950	27
RR+	$7.52 \times 10^8$	6215	467	$7.52 \times 10^8$	7655	1062
RR-	$7.52 \times 10^8$	1179	4	$7.52 \times 10^8$	1240	30
LR+	$7.52 \times 10^8$	6215	1594	$7.52 \times 10^8$	7025	2075
LR-	$7.52 \times 10^8$	1179	48	$7.52 \times 10^8$	1333	106
RL+	$7.52 \times 10^8$	6215	847	$7.52 \times 10^8$	6965	1219
RL-	$7.52 \times 10^8$	6215	48	$7.52 \times 10^8$	6325	104

$\Lambda = 30$  TeV;  $\mathcal{L}_{\text{int}} = 50 \text{ fb}^{-1}$

## 5. Significance calculation for compositeness scale

In this section, the calculation results for the exclusion ( $2\sigma$ ), observation ( $3\sigma$ ), and discovery ( $5\sigma$ ) limits on the compositeness scale in contact interactions at FCC-based muon–proton colliders are given. For this, we used Eq. (6) to obtain statistical significance calculation for both constructive and destructive interferences

$$\text{Significance} = \frac{\sigma_{(\text{CI+SM})} - \sigma_{(\text{SM})}}{\sqrt{\sigma_{(\text{SM})}}} \sqrt{\mathcal{L}_{\text{int}}}. \quad (6)$$

Here,  $\sigma_{(\text{CI+SM})}$  denotes the Contact and Standard Model interactions cross section as a signal,  $\sigma_{(\text{SM})}$  represents the Standard Model cross section as a background, and  $\mathcal{L}_{\text{int}}$  is the integrated luminosity of the  $\mu p$  colliders. The statistical uncertainties in our calculations were due to uncertainty in the integrated luminosity.  $\delta\mathcal{L}/\mathcal{L} = 1/\sqrt{\mathcal{L}}$  equality scales the sensitivity of the integrated luminosity [87, 88]. Therefore, using this sensitivity in our significance calculations, we calculated the statistical uncertainties in the compositeness scale.

Using the relevant cut sets in Table 2 and Eq. (6), the exclusion, observation, and discovery limits of the compositeness scale for all constructive and destructive interferences ( $A_{\text{LL}}^+$ ,  $A_{\text{LL}}^-$ ,  $A_{\text{RR}}^+$ ,  $A_{\text{RR}}^-$ ,  $A_{\text{LR}}^+$ ,  $A_{\text{LR}}^-$ ,  $A_{\text{RL}}^+$ , and  $A_{\text{RL}}^-$ ) for the final luminosity value of  $50 \text{ fb}^{-1}$  at the muon–proton collider with the center-of-mass energy  $\sqrt{s} = 12.2$  TeV are given in Fig. 5. It is seen that  $A_{\text{LL}}^+$  has the highest compositeness scale limits and  $A_{\text{RL}}^-$  has the lowest.

The compositeness scale values with sensitivity lie between  $33.2 \pm 1.5\%$  TeV and  $56.5 \pm 2.7\%$  TeV for the discovery,  $36.9 \pm 1.4\%$  TeV and  $69.7 \pm 2.9\%$  TeV for observation, and  $40.1 \pm 1.4\%$  TeV and  $83.2 \pm 3.0\%$  TeV for exclusion. These limits are far beyond the LHC experimental results. The compositeness scale limits in terms of luminosities are given in Table 4 for the rest of the helicities with constructive and destructive interferences.

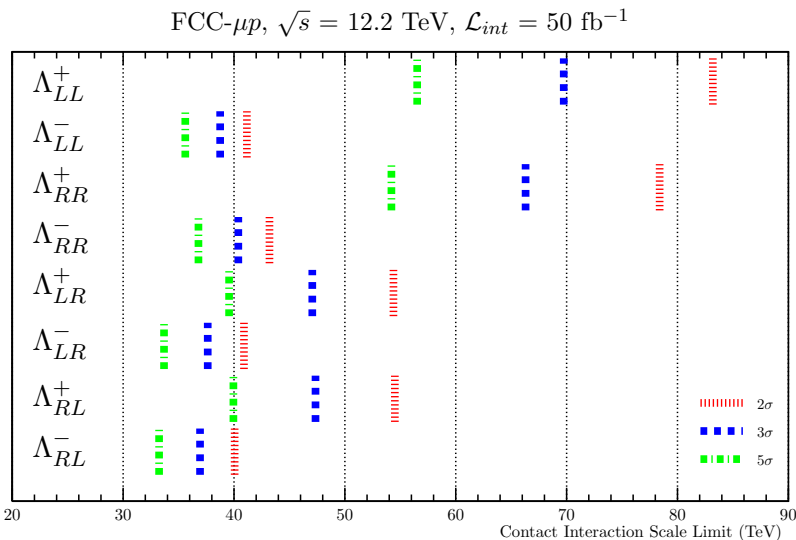


Fig. 5. Contact interactions scale limits for the FCC-based muon-proton collider with  $\sqrt{s} = 12.2$  TeV at  $\mathcal{L}_{int} = 50$  fb $^{-1}$ .

Table 4. Attainable limits on the compositeness scales with sensitivity at the FCC-based  $\mu p$  collider with  $\sqrt{s} = 12.2$  TeV for the first, the fifth, and the tenth years' luminosities.

$\mu 750 \otimes \text{FCC}$		$A \pm \delta\%$ [TeV]							
$\mathcal{L}_{int}$	C.L.	$A_{LL}^+$	$A_{LL}^-$	$A_{RR}^+$	$A_{RR}^-$	$A_{LR}^+$	$A_{LR}^-$	$A_{RL}^+$	$A_{RL}^-$
5	5 $\sigma$	$37.0 \pm 4.2\%$	$28.4 \pm 2.8\%$	$35.5 \pm 4.4\%$	$29.0 \pm 2.7\%$	$27.7 \pm 3.7\%$	$25.9 \pm 3.0\%$	$28.2 \pm 3.6\%$	$25.7 \pm 2.7\%$
	3 $\sigma$	$44.3 \pm 4.5\%$	$31.6 \pm 2.5\%$	$42.6 \pm 4.5\%$	$32.4 \pm 2.6\%$	$32.3 \pm 3.8\%$	$29.2 \pm 2.8\%$	$32.8 \pm 3.8\%$	$28.9 \pm 2.8\%$
	2 $\sigma$	$51.5 \pm 4.7\%$	$34.1 \pm 2.3\%$	$49.5 \pm 4.6\%$	$35.2 \pm 2.5\%$	$36.7 \pm 3.9\%$	$32.0 \pm 2.8\%$	$37.1 \pm 3.9\%$	$31.6 \pm 2.8\%$
25	5 $\sigma$	$49.4 \pm 3.1\%$	$33.5 \pm 1.5\%$	$47.5 \pm 3.0\%$	$34.4 \pm 1.7\%$	$35.4 \pm 2.6\%$	$31.2 \pm 1.9\%$	$35.8 \pm 2.4\%$	$30.9 \pm 1.8\%$
	3 $\sigma$	$60.4 \pm 3.3\%$	$36.6 \pm 1.4\%$	$57.8 \pm 3.2\%$	$37.9 \pm 1.5\%$	$41.8 \pm 2.7\%$	$34.9 \pm 1.8\%$	$42.1 \pm 2.7\%$	$34.4 \pm 1.7\%$
	2 $\sigma$	$71.5 \pm 3.5\%$	$39.1 \pm 1.3\%$	$67.9 \pm 3.3\%$	$40.8 \pm 1.4\%$	$48.0 \pm 2.9\%$	$38.1 \pm 1.7\%$	$48.3 \pm 2.8\%$	$37.4 \pm 1.7\%$
50	5 $\sigma$	$56.5 \pm 2.7\%$	$35.6 \pm 1.2\%$	$54.2 \pm 2.6\%$	$36.8 \pm 1.3\%$	$39.6 \pm 2.2\%$	$33.7 \pm 1.5\%$	$39.9 \pm 2.2\%$	$33.2 \pm 1.5\%$
	3 $\sigma$	$69.7 \pm 2.9\%$	$38.7 \pm 1.1\%$	$66.3 \pm 2.8\%$	$40.4 \pm 1.2\%$	$47.0 \pm 2.4\%$	$37.6 \pm 1.4\%$	$47.4 \pm 2.3\%$	$36.9 \pm 1.4\%$
	2 $\sigma$	$83.2 \pm 3.0\%$	$41.2 \pm 1.0\%$	$78.4 \pm 2.9\%$	$43.2 \pm 1.1\%$	$54.4 \pm 2.5\%$	$40.9 \pm 1.4\%$	$54.5 \pm 2.4\%$	$40.1 \pm 1.4\%$

As mentioned above, we used the relevant cut sets in Table 2 and equation (6) to calculate statistical significances for the other two collider options with 17.3 and 24.5 TeV center-of-mass energies. Figures 6 and 7 show the

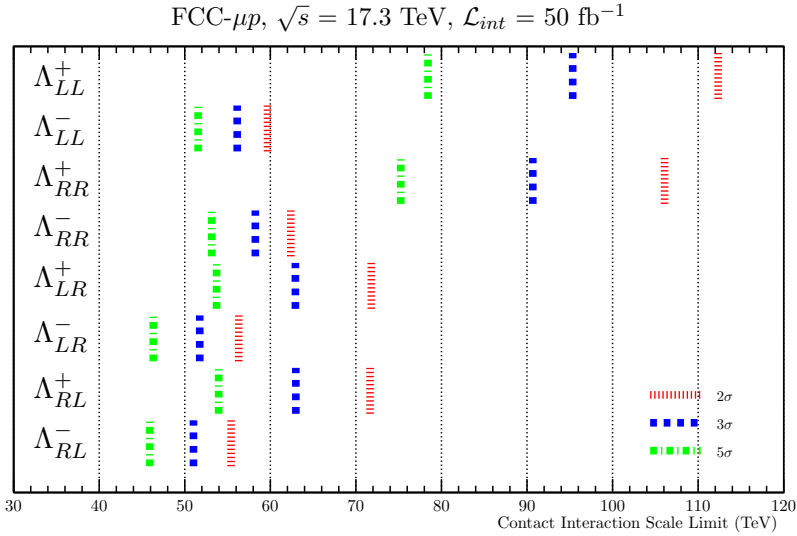


Fig. 6. Contact interactions scale limits for the FCC-based muon-proton collider with  $\sqrt{s} = 17.3$  TeV at  $\mathcal{L}_{int} = 50$  fb $^{-1}$ .

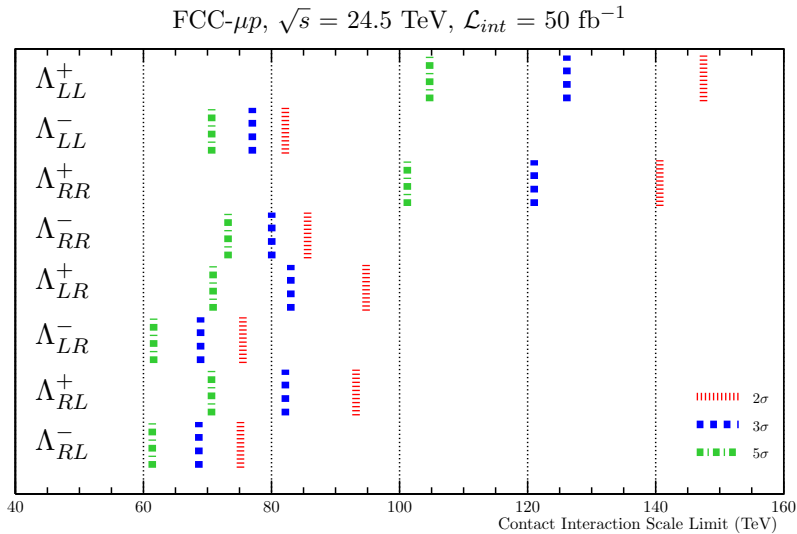


Fig. 7. Contact interactions scale limits for the FCC-based muon-proton collider with  $\sqrt{s} = 24.5$  TeV at  $\mathcal{L}_{int} = 50$  fb $^{-1}$ .

compositeness scale limits for all constructive and destructive interferences, respectively. The highest limit is achieved for  $A_{LL}^+$ , and the lowest limit is achieved for  $A_{RL}^-$  in both collider options. As seen in Fig. 6, discovery limits show variation between  $45.9 \pm 1.4\%$  TeV and  $78.4 \pm 2.5\%$  TeV; observation limits are between  $51.0 \pm 1.4\%$  TeV and  $95.3 \pm 2.7\%$  TeV; exclusion limits swing from  $55.4 \pm 1.4\%$  TeV to  $112.3 \pm 2.8\%$  TeV. In Table 6, the highest and the lowest discovery, observation, and exclusion limits are  $(104.7 \pm 2.4\% : 61.4 \pm 1.5\%)$  TeV,  $(126.1 \pm 2.6\% : 68.6 \pm 1.5\%)$  TeV, and  $(147.5 \pm 2.7\% : 75.2 \pm 1.5\%)$  TeV for the  $\mu 3000 \otimes \text{FCC}$  option with  $50 \text{ fb}^{-1}$  integrated luminosity, respectively. Tables 5 and 6 give detailed compositeness scale limit results with their sensitivities for both  $\mu p$  colliders.

Table 5. Attainable limits on the compositeness scales with sensitivity at the FCC-based  $\mu p$  collider with  $\sqrt{s} = 17.3$  TeV for the first, the fifth, and the tenth years' luminosities.

$\mu 1500 \otimes \text{FCC}$		$A \pm \delta\%$ [TeV]							
$\mathcal{L}_{\text{int}}$	C.L.	$A_{LL}^+$	$A_{LL}^-$	$A_{RR}^+$	$A_{RR}^-$	$A_{LR}^+$	$A_{LR}^-$	$A_{RL}^+$	$A_{RL}^-$
5	$5\sigma$	$52.7 \pm 4.0\%$	$41.3 \pm 2.7\%$	$51.4 \pm 3.9\%$	$42.0 \pm 2.9\%$	$38.4 \pm 3.6\%$	$35.8 \pm 3.1\%$	$38.9 \pm 3.5\%$	$35.6 \pm 3.0\%$
	$3\sigma$	$62.4 \pm 4.2\%$	$45.8 \pm 2.4\%$	$60.5 \pm 4.0\%$	$46.9 \pm 2.6\%$	$44.4 \pm 3.6\%$	$40.4 \pm 2.9\%$	$44.9 \pm 3.5\%$	$40.0 \pm 2.8\%$
	$2\sigma$	$72.0 \pm 4.4\%$	$49.4 \pm 2.3\%$	$69.3 \pm 4.2\%$	$50.8 \pm 2.4\%$	$50.1 \pm 3.7\%$	$44.2 \pm 2.7\%$	$50.4 \pm 3.6\%$	$43.7 \pm 2.7\%$
25	$5\sigma$	$69.2 \pm 2.9\%$	$48.4 \pm 1.5\%$	$66.7 \pm 2.8\%$	$49.8 \pm 1.6\%$	$48.4 \pm 2.4\%$	$43.2 \pm 1.8\%$	$48.8 \pm 2.3\%$	$42.7 \pm 1.8\%$
	$3\sigma$	$83.4 \pm 3.1\%$	$52.9 \pm 1.4\%$	$79.8 \pm 2.9\%$	$54.8 \pm 1.5\%$	$56.5 \pm 2.5\%$	$48.2 \pm 1.7\%$	$56.7 \pm 2.4\%$	$47.5 \pm 1.7\%$
	$2\sigma$	$97.6 \pm 3.2\%$	$56.5 \pm 1.3\%$	$92.7 \pm 3.1\%$	$58.8 \pm 1.4\%$	$64.1 \pm 2.6\%$	$52.3 \pm 1.7\%$	$64.1 \pm 2.5\%$	$51.6 \pm 1.7\%$
50	$5\sigma$	$78.4 \pm 2.5\%$	$51.5 \pm 1.2\%$	$75.2 \pm 2.4\%$	$53.1 \pm 1.3\%$	$53.7 \pm 2.1\%$	$46.5 \pm 1.5\%$	$54.0 \pm 2.0\%$	$45.9 \pm 1.4\%$
	$3\sigma$	$95.3 \pm 2.7\%$	$56.0 \pm 1.1\%$	$90.7 \pm 2.6\%$	$58.2 \pm 1.2\%$	$62.9 \pm 2.2\%$	$51.7 \pm 1.4\%$	$63.0 \pm 2.1\%$	$51.0 \pm 1.4\%$
	$2\sigma$	$112.3 \pm 2.8\%$	$59.6 \pm 1.0\%$	$106.1 \pm 2.7\%$	$62.4 \pm 1.1\%$	$71.8 \pm 2.3\%$	$56.1 \pm 1.4\%$	$71.7 \pm 2.2\%$	$55.4 \pm 1.4\%$

Table 6. Attainable limits on the compositeness scales with sensitivity at the FCC-based  $\mu p$  collider with  $\sqrt{s} = 24.5$  TeV for the first, the fifth, and the tenth years' luminosities.

$\mu 3000 \otimes \text{FCC}$		$A \pm \delta\%$ [TeV]							
$\mathcal{L}_{\text{int}}$	C.L.	$A_{LL}^+$	$A_{LL}^-$	$A_{RR}^+$	$A_{RR}^-$	$A_{LR}^+$	$A_{LR}^-$	$A_{RL}^+$	$A_{RL}^-$
5	$5\sigma$	$71.4 \pm 3.9\%$	$56.8 \pm 2.6\%$	$70.0 \pm 3.8\%$	$58.5 \pm 2.7\%$	$50.9 \pm 3.5\%$	$47.8 \pm 2.8\%$	$51.1 \pm 3.4\%$	$47.5 \pm 2.9\%$
	$3\sigma$	$84.2 \pm 4.1\%$	$62.9 \pm 2.4\%$	$82.0 \pm 3.9\%$	$65.0 \pm 2.5\%$	$58.8 \pm 3.5\%$	$53.5 \pm 2.8\%$	$58.9 \pm 3.5\%$	$53.3 \pm 2.8\%$
	$2\sigma$	$96.5 \pm 4.2\%$	$67.8 \pm 2.3\%$	$93.5 \pm 4.1\%$	$70.1 \pm 2.3\%$	$66.1 \pm 3.6\%$	$58.5 \pm 2.7\%$	$66.0 \pm 3.5\%$	$58.3 \pm 2.7\%$
25	$5\sigma$	$92.8 \pm 2.8\%$	$66.4 \pm 1.5\%$	$90.2 \pm 2.7\%$	$68.7 \pm 1.5\%$	$64.0 \pm 2.4\%$	$57.1 \pm 1.8\%$	$64.0 \pm 2.3\%$	$56.9 \pm 1.8\%$
	$3\sigma$	$111.0 \pm 2.9\%$	$72.7 \pm 1.4\%$	$107.1 \pm 2.8\%$	$75.4 \pm 1.5\%$	$74.5 \pm 2.5\%$	$63.8 \pm 1.8\%$	$74.1 \pm 2.4\%$	$63.6 \pm 1.8\%$
	$2\sigma$	$129.0 \pm 3.1\%$	$77.7 \pm 1.3\%$	$123.6 \pm 3.0\%$	$80.8 \pm 1.4\%$	$84.6 \pm 2.6\%$	$69.8 \pm 1.8\%$	$83.7 \pm 2.5\%$	$69.5 \pm 1.8\%$
50	$5\sigma$	$104.7 \pm 2.4\%$	$70.7 \pm 1.2\%$	$101.2 \pm 2.3\%$	$73.2 \pm 1.2\%$	$70.9 \pm 2.1\%$	$61.6 \pm 1.5\%$	$70.6 \pm 2.0\%$	$61.4 \pm 1.5\%$
	$3\sigma$	$126.1 \pm 2.6\%$	$77.0 \pm 1.1\%$	$121.0 \pm 2.5\%$	$80.0 \pm 1.2\%$	$83.0 \pm 2.2\%$	$68.9 \pm 1.5\%$	$82.2 \pm 2.1\%$	$68.6 \pm 1.5\%$
	$2\sigma$	$147.5 \pm 2.7\%$	$82.2 \pm 1.1\%$	$140.6 \pm 2.6\%$	$85.6 \pm 1.1\%$	$94.8 \pm 2.3\%$	$75.5 \pm 1.6\%$	$93.2 \pm 2.2\%$	$75.2 \pm 1.5\%$

Regarding the last collider option in Table 1 with the 63.2 TeV center-of-mass energy, Fig. 8 depicts the same pattern as other collider options that the lowest compositeness scale limits are revealed for  $\Lambda_{RL}^-$ , and the highest compositeness scale limits appeared for  $\Lambda_{LL}^+$ , at all confidence levels. The final integrated luminosity value is  $100 \text{ fb}^{-1}$  for the  $\mu 20000 \otimes \text{FCC}$  collider at the end of the ten years. The highest discovery, observation, and exclusion

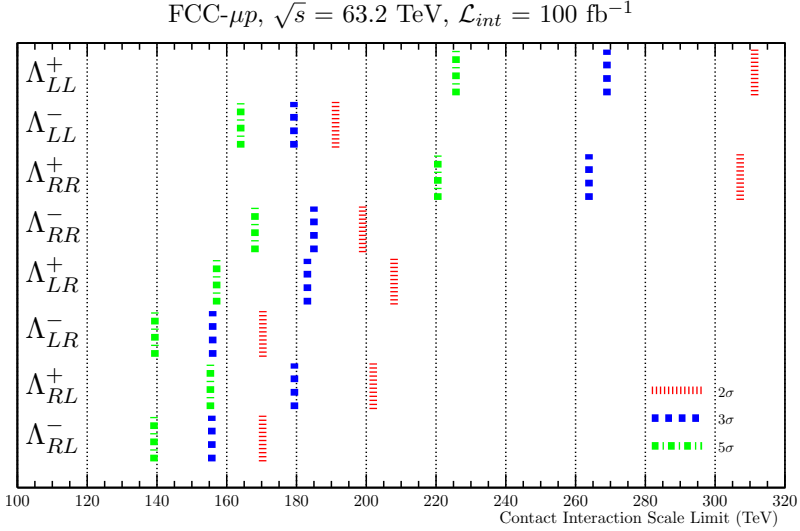


Fig. 8. Contact interactions scale limits for the FCC-based muon-proton collider with  $\sqrt{s} = 63.2 \text{ TeV}$  at  $\mathcal{L}_{int} = 100 \text{ fb}^{-1}$ .

Table 7. Attainable limits on the compositeness scales with sensitivity at the FCC-based  $\mu p$  collider with  $\sqrt{s} = 63.2 \text{ TeV}$  for the first, the fifth, and the tenth years' luminosities.

$\mu 20000 \otimes \text{FCC}$		$\Lambda \pm \delta\%$ [TeV]								
$\mathcal{L}_{int}$ [ $\text{fb}^{-1}$ ]	C.L.	$\Lambda_{LL}^+$	$\Lambda_{LL}^-$	$\Lambda_{RR}^+$	$\Lambda_{RR}^-$	$\Lambda_{LR}^+$	$\Lambda_{LR}^-$	$\Lambda_{RL}^+$	$\Lambda_{RL}^-$	
	5 $\sigma$	$157.0 \pm 2.9\%$	$130.3 \pm 2.4\%$	$153.8 \pm 3.0\%$	$132.0 \pm 2.4\%$	$113.0 \pm 2.9\%$	$106.4 \pm 2.6\%$	$113.1 \pm 2.9\%$	$106.8 \pm 2.5\%$	
	10	3 $\sigma$	$183.6 \pm 3.2\%$	$144.8 \pm 2.1\%$	$179.2 \pm 3.2\%$	$147.7 \pm 2.2\%$	$130.6 \pm 2.9\%$	$120.4 \pm 2.5\%$	$130.2 \pm 2.8\%$	$120.5 \pm 2.4\%$
	2 $\sigma$	$208.9 \pm 3.3\%$	$156.8 \pm 2.0\%$	$203.9 \pm 3.4\%$	$160.5 \pm 2.1\%$	$146.7 \pm 3.0\%$	$132.2 \pm 2.4\%$	$145.5 \pm 2.9\%$	$132.1 \pm 2.3\%$	
50	5 $\sigma$	$201.5 \pm 2.2\%$	$153.5 \pm 1.3\%$	$196.6 \pm 2.2\%$	$157.0 \pm 1.4\%$	$142.1 \pm 2.0\%$	$128.9 \pm 1.6\%$	$141.1 \pm 1.9\%$	$128.8 \pm 1.6\%$	
	3 $\sigma$	$238.5 \pm 2.3\%$	$168.9 \pm 1.2\%$	$233.3 \pm 2.4\%$	$173.4 \pm 1.3\%$	$164.9 \pm 2.0\%$	$144.6 \pm 1.5\%$	$162.6 \pm 1.9\%$	$144.3 \pm 1.5\%$	
	2 $\sigma$	$274.7 \pm 2.4\%$	$181.1 \pm 1.1\%$	$269.6 \pm 2.5\%$	$187.0 \pm 1.3\%$	$186.5 \pm 2.1\%$	$158.0 \pm 1.5\%$	$182.5 \pm 2.0\%$	$157.7 \pm 1.5\%$	
100	5 $\sigma$	$225.7 \pm 1.9\%$	$163.9 \pm 1.1\%$	$220.5 \pm 1.9\%$	$168.1 \pm 1.1\%$	$157.1 \pm 1.7\%$	$139.4 \pm 1.3\%$	$155.3 \pm 1.6\%$	$139.1 \pm 1.3\%$	
	3 $\sigma$	$269.0 \pm 2.0\%$	$179.3 \pm 1.0\%$	$263.8 \pm 2.1\%$	$185.0 \pm 1.1\%$	$183.1 \pm 1.8\%$	$156.0 \pm 1.3\%$	$179.4 \pm 1.6\%$	$155.7 \pm 1.3\%$	
	2 $\sigma$	$311.3 \pm 2.1\%$	$191.3 \pm 0.9\%$	$307.2 \pm 2.2\%$	$199.0 \pm 1.0\%$	$208.0 \pm 1.8\%$	$170.4 \pm 1.3\%$	$202.0 \pm 1.7\%$	$170.3 \pm 1.3\%$	

limits are obtained as  $225.7 \pm 1.9\%$  TeV,  $269.0 \pm 2.0\%$  TeV, and  $311.3 \pm 2.1\%$  TeV with constructive  $A_{LL}^+$ , and the lowest limits of confidence levels are achieved as  $139.1 \pm 1.3\%$  TeV,  $155.7 \pm 1.3\%$  TeV, and  $170.3 \pm 1.3\%$  TeV with destructive  $A_{RL}^-$ , respectively. Table 7 lists detailed compositeness scale limits with sensitivity for all confidence levels at  $\mu 20000 \otimes \text{FCC}$  collider.

## 6. Conclusion

We carried out a contact interaction study at FCC-based muon–proton colliders. In our calculations, we considered four center-of-mass energies  $\mu p$  collider options. The FCC-based  $\mu p$  collider of the highest center-of-mass energy (63.2 TeV) option with the luminosity  $100 \text{ fb}^{-1}$  reveals the largest attainable compositeness scales. This machine will allow for discovery up to  $225.7 \pm 1.9\%$  TeV, observation  $269.0 \pm 2.0\%$  TeV, and exclusion  $311.3 \pm 2.1\%$  TeV for  $A_{LL}^+$  (constructive interference) in four-fermion contact interactions. When we consider destructive interference for the left–left helicity at this collider, discovery, observation, and exclusion limits are calculated as  $163.9 \pm 1.1\%$  TeV,  $179.3 \pm 1.0\%$  TeV, and  $191.3 \pm 0.9\%$  TeV, respectively. As can be seen from Ref. [89] for  $pp \rightarrow jj$  process, it has been demonstrated that in the future proton–proton colliders, with an integrated luminosity value of  $3000 \text{ fb}^{-1}$ , an exclusion limit of approximately 45 TeV can be imposed on the compositeness scale (LL, RR) by contact interactions in the 33 TeV center-of-mass energy option. With the same integrated luminosity value, for the option with a center-of-mass energy of 100 TeV, an exclusion limit of 125 TeV was envisaged to be put on the compositeness scale. In addition to these options, High Luminosity Large Hadron Collider ( $\mathcal{L}_{\text{int}} = 3000 \text{ fb}^{-1}$ ) projects exclusion limits on a compositeness scale around 60 TeV via  $pp \rightarrow ll$  process in contact interactions [85]. As shown in Table 6, the limit imposed on the compositeness scale is higher in the muon–proton collider in our study with a 24.5 TeV center of mass-energy and  $50 \text{ fb}^{-1}$  integrated luminosity. Moreover, the muon–proton collider option with  $100 \text{ fb}^{-1}$  integrated luminosity with 63.5 TeV center-of-mass energy can also introduce a higher exclusion limit to the compositeness scale than the 100 TeV center-of-mass collider in Ref. [89]. In addition, the compositeness scale could be examined up to 100 TeV for contact interactions in the FCC-eh collider [57]. We indicated that FCC- $\mu p$  colliders could push the limits of the compositeness scale in contact interactions higher than Refs. [57] and [89]. Our findings show that FCC-based muon–proton colliders have greater potential regarding four-fermion contact interactions than LHC, ILC, CLIC, HL-LHC, FCC-eh, and future  $pp$  colliders. As a result, FCC-based  $\mu p$  colliders will be an exceptional alternative for researching four-fermion contact interactions.

The authors are obliged to the Usak University Energy, Environment, and Sustainability Application and Research Center for support. Figures in this paper are created using the ROOT software [90].

## REFERENCES

- [1] J.C. Pati, A. Salam, «Lepton number as the fourth “color”», *Phys. Rev. D* **10**, 275 (1974); *Erratum ibid.* **11**, 703 (1975).
- [2] H. Terazawa, Y. Chikashige, K. Akama, «Unified model of the Nambu–Jona-Lasinio type for all elementary-particle forces», *Phys. Rev. D* **15**, 480 (1977).
- [3] H. Harari, «A schematic model of quarks and leptons», *Phys. Lett. B* **86**, 83 (1979).
- [4] M. Shupe, «A composite model of leptons and quarks», *Phys. Lett. B* **86**, 87 (1979).
- [5] H. Terazawa, «Subquark model of leptons and quarks», *Phys. Rev. D* **22**, 184 (1980).
- [6] H. Fritzsch, G. Mandelbaum, «Weak interactions as manifestations of the substructure of leptons and quarks», *Phys. Lett. B* **102**, 319 (1981).
- [7] H. Terazawa, M. Yasuè, K. Akama, M. Hayashi, «Observable effects of the possible sub-structure of leptons and quarks», *Phys. Lett. B* **112**, 387 (1982).
- [8] E.J. Eichten, K.D. Lane, M.E. Peskin, «New Tests for Quark and Lepton Substructure», *Phys. Rev. Lett.* **50**, 811 (1983).
- [9] L. Lyons, «An introduction to the possible substructure of quarks and leptons», *Prog. Part. Nucl. Phys.* **10**, 227 (1983).
- [10] H. Terazawa, «A fundamental theory of composite particles and fields», *Phys. Lett. B* **133**, 57 (1983).
- [11] I.A. D’Souza, C.S. Kalman, «Preons: Models of Leptons, Quarks and Gauge Bosons as Composite Objects», *World Scientific*, 1992.
- [12] A. Çelikel, M. Kantar, S. Sultansoy, «A search for sextet quarks and leptogluons at the LHC», *Phys. Lett. B* **443**, 359 (1998).
- [13] M.E. de Souza, «Weak decays of hadrons reveal compositeness of quarks», *Scientia Plena* **4**, 6 (2008).
- [14] H. Terazawa, M. Yasuè, «Composite Higgs Boson in the Unified Subquark Model of all Fundamental Particles and Forces», *J. Mod. Phys.* **05**, 205 (2014).
- [15] H. Fritzsch, «Composite weak bosons at the large hadronic collider», *Mod. Phys. Lett. A* **31**, 1630019 (2016).
- [16] H. Terazawa, M. Yasuè, «Excited Gauge and Higgs Bosons in the Unified Composite Model», *Nonlin. Phenom. Complex Syst.* **19**, 1 (2016).
- [17] U. Kaya, B.B. Öner, S. Sultanoğlu, «A minimal fermion-scalar preonic model», *Turk. J. Phys.* **42**, 235 (2018).

- [18] E. Eichten, I. Hinchliffe, K. Lane, C. Quigg, «Supercollider physics», *Rev. Mod. Phys.* **56**, 579 (1984).
- [19] W. Buchmüller, B. Lampe, N. Vlachos, «Contact interactions and the Callan–Gross relation», *Phys. Lett. B* **197**, 379 (1987).
- [20] B. Schrempp, F. Schrempp, N. Wermes, D. Zeppenfeld, «Bounds on new contact interactions from future  $e^+e^-$  colliders», *Nucl. Phys. B* **296**, 1 (1988).
- [21] E.N. Argyres, O. Korakianitis, C.G. Papadopoulos, S.D.P. Vlassopoulos, «Accompanied dileptons as a probe of an effective quark–lepton contact interaction at  $e^+e^-$  colliders», *Nucl. Phys. B* **354**, 1 (1991).
- [22] T.G. Rizzo, «Diphoton production at hadron colliders and new contact interactions», *Phys. Rev. D* **51**, 1064 (1995).
- [23] V. Barger, K. Cheung, K. Hagiwara, D. Zeppenfeld, «Global study of electron–quark contact interactions», *Phys. Rev. D* **57**, 391 (1998).
- [24] K. Cheung, «Muon–proton colliders: Leptoquarks and contact interactions», *AIP Conf. Proc.* **441**, 338 (1998).
- [25] A. Žarnecki, «Global analysis of  $eeqq$  contact interactions and future prospects for high energy physics», *Eur. Phys. J. C* **11**, 539 (1999).
- [26] A.A. Babich, P. Osland, A.A. Pankov, N. Paver, «Contact interactions and polarized beams at a linear collider», Technical Report LC-TH-2001-021, BERGEN-2001-01, [arXiv:hep-ph/0101150](https://arxiv.org/abs/hep-ph/0101150).
- [27] Particle Data Group (P.A. Zyla *et al.*), «Review of Particle Physics», *Prog. Theor. Exp. Phys.* **2020**, 083C01 (2020).
- [28] ALEPH Collaboration (S. Schael *et al.*), «Fermion pair production in  $e^+e^-$  collisions at 189–209 GeV and constraints on physics beyond the standard model», *Eur. Phys. J. C* **49**, 411 (2006).
- [29] DELPHI Collaboration (J. Abdallah *et al.*), «Measurement and interpretation of fermion-pair production at LEP energies above the  $Z$  resonance», *Eur. Phys. J. C* **45**, 589 (2006).
- [30] DELPHI Collaboration (J. Abdallah *et al.*), «A study of  $b\bar{b}$  production in  $e^+e^-$  collisions at  $\sqrt{s} = 130\text{--}207$  GeV», *Eur. Phys. J. C* **60**, 1 (2009).
- [31] L3 Collaboration (M. Acciarri *et al.*), «Search for manifestations of new physics in fermion-pair production at LEP», *Phys. Lett. B* **489**, 81 (2000).
- [32] OPAL Collaboration (G. Abbiendi *et al.*), «Tests of the standard model and constraints on new physics from measurements of fermion-pair production at 189–209 GeV at LEP», *Eur. Phys. J. C* **33**, 173 (2004).
- [33] H1 Collaboration (F. Aaron *et al.*), «Search for contact interactions in  $e^\pm p$  collisions at HERA», *Phys. Lett. B* **705**, 52 (2011).
- [34] ZEUS Collaboration (S. Chekanov *et al.*), «Search for contact interactions, large extra dimensions and finite quark radius in  $ep$  collisions at HERA», *Phys. Lett. B* **591**, 23 (2004).

- [35] CDF Collaboration (F. Abe *et al.*), «Limits on Quark–Lepton Compositeness Scales from Dileptons Produced in 1.8 TeV  $p\bar{p}$  Collisions», *Phys. Rev. Lett.* **79**, 2198 (1997).
- [36] CDF Collaboration (T. Affolder *et al.*), «Search for Quark–Lepton Compositeness and a Heavy  $W'$  Boson Using the  $e\nu$  Channel in  $p\bar{p}$  Collisions at  $\sqrt{s} = 1.8$  TeV», *Phys. Rev. Lett.* **87**, 231803 (2001).
- [37] CDF Collaboration (A. Abulencia *et al.*), «Search for  $Z' \rightarrow e^+e^-$  Using Dielectron Mass and Angular Distribution», *Phys. Rev. Lett.* **96**, 211801 (2006).
- [38] D0 Collaboration (B. Abbott *et al.*), «Measurement of the High-Mass Drell–Yan Cross Section and Limits on Quark–Electron Compositeness Scales», *Phys. Rev. Lett.* **82**, 4769 (1999).
- [39] D0 Collaboration (V.M. Abazov *et al.*), «Measurement of Dijet Angular Distributions at  $\sqrt{s} = 1.96$  TeV and Searches for Quark Compositeness and Extra Spatial Dimensions», *Phys. Rev. Lett.* **103**, 191803 (2009).
- [40] ATLAS Collaboration (G. Aad *et al.*), «Search for quark contact interactions in dijet angular distributions in  $pp$  collisions at  $s = 7$  TeV measured with the ATLAS detector», *Phys. Lett. B* **694**, 327 (2011).
- [41] ATLAS Collaboration (G. Aad *et al.*), «A search for new physics in dijet mass and angular distributions in  $pp$  collisions at  $\sqrt{s} = 7$  TeV measured with the ATLAS detector», *New J. Phys.* **13**, 053044 (2011).
- [42] ATLAS Collaboration (G. Aad *et al.*), «ATLAS search for new phenomena in dijet mass and angular distributions using  $pp$  collisions at  $\sqrt{s} = 7$  TeV», *J. High Energy Phys.* **2013**, 29 (2013).
- [43] ATLAS Collaboration (G. Aad *et al.*), «Search for contact interactions and large extra dimensions in the dilepton channel using proton–proton collisions at  $\sqrt{s} = 8$  TeV with the ATLAS detector», *Eur. Phys. J. C* **74**, 3134 (2014).
- [44] ATLAS Collaboration (G. Aad *et al.*), «Search for New Phenomena in Dijet Angular Distributions in Proton–Proton Collisions at  $\sqrt{s} = 8$  TeV Measured with the ATLAS Detector», *Phys. Rev. Lett.* **114**, 221802 (2015).
- [45] ATLAS Collaboration (G. Aad *et al.*), «Search for new phenomena in dijet mass and angular distributions from  $pp$  collisions at  $\sqrt{s} = 13$  TeV with the ATLAS detector», *Phys. Lett. B* **754**, 302 (2016).
- [46] ATLAS Collaboration (M. Aaboud *et al.*), «Search for new phenomena in dijet events using  $37 \text{ fb}^{-1}$  of  $pp$  collision data collected at  $\sqrt{s} = 13$  TeV with the ATLAS detector», *Phys. Rev. D* **96**, 052004 (2017).
- [47] CMS Collaboration (V. Khachatryan *et al.*), «Search for Quark Compositeness with the Dijet Centrality Ratio in  $pp$  Collisions at  $\sqrt{s} = 7$  TeV», *Phys. Rev. Lett.* **105**, 262001 (2010).
- [48] CMS Collaboration (V. Khachatryan *et al.*), «Measurement of Dijet Angular Distributions and Search for Quark Compositeness in  $pp$  Collisions at  $\sqrt{s} = 7$  TeV», *Phys. Rev. Lett.* **106**, 201804 (2011).

- [49] CMS Collaboration (S. Chatrchyan *et al.*), «Search for quark compositeness in dijet angular distributions from  $pp$  collisions at  $\sqrt{s} = 7$  TeV», *J. High Energy Phys.* **2012**, 55 (2012).
- [50] CMS Collaboration (V. Khachatryan *et al.*), «Search for quark contact interactions and extra spatial dimensions using dijet angular distributions in proton–proton collisions at  $\sqrt{s} = 8$  TeV», *Phys. Lett. B* **746**, 79 (2015).
- [51] CMS Collaboration (S. Chatrchyan *et al.*), «Search for contact interactions using the inclusive jet  $p_T$  spectrum in  $pp$  collisions at  $\sqrt{s} = 7$  TeV», *Phys. Rev. D* **87**, 052017 (2013).
- [52] CMS Collaboration (A.M. Sirunyan *et al.*), «Search for new physics with dijet angular distributions in proton–proton collisions at  $\sqrt{s} = 13$  TeV», *J. High Energy Phys.* **2017**, 13 (2017).
- [53] CMS Collaboration (A.M. Sirunyan *et al.*), «Search for new physics in dijet angular distributions using proton–proton collisions at  $\sqrt{s} = 13$  TeV and constraints on dark matter and other models», *Eur. Phys. J. C* **78**, 789 (2018).
- [54] ATLAS Collaboration (M. Aaboud *et al.*), «Search for new high-mass phenomena in the dilepton final state using  $36 \text{ fb}^{-1}$  of proton–proton collision data at  $\sqrt{s} = 13$  TeV with the ATLAS detector», *J. High Energy Phys.* **2017**, 182 (2017).
- [55] FCC Collaboration (A. Abada *et al.*), «FCC Phys. Opportunities: Future Circular Collider Conceptual Design Report Volume 1», *Eur. Phys. J. C* **79**, 474 (2019).
- [56] FCC Collaboration (A. Abada *et al.*), «FCC-ee: The Lepton Collider: Future Circular Collider Conceptual Design Report Volume 2», *Eur. Phys. J. Spec. Top.* **228**, 261 (2019).
- [57] FCC Collaboration (A. Abada *et al.*), «FCC-hh: The Hadron Collider: Future Circular Collider Conceptual Design Report Volume 3», *Eur. Phys. J. Spec. Top.* **228**, 755 (2019).
- [58] FCC Collaboration (A. Abada *et al.*), «HE-LHC: The High-Energy Large Hadron Collider: Future Circular Collider Conceptual Design Report Volume 4», *Eur. Phys. J. Spec. Top.* **228**, 1109 (2019).
- [59] D. Neuffer, «Principles and Applications of Muon Cooling», *Part. Accel.* **14**, 75 (1983).
- [60] M. Antonelli, M. Boscolo, R. Di Nardo, P. Raimondi, «Novel proposal for a low emittance muon beam using positron beam on target», *Nucl. Instrum. Methods Phys. Res. A* **807**, 101 (2016).
- [61] F. Zimmermann, «LHC/FCC-based muon colliders», *J. Phys.: Conf. Ser.* **1067**, 022017 (2018).
- [62] D. Neuffer, V. Shiltsev, «On the feasibility of a pulsed 14 TeV c.m.e. muon collider in the LHC tunnel», *J. Instrum.* **13**, T10003 (2018).
- [63] M. Boscolo, J.-P. Delahaye, M. Palmer, «The future prospects of muon colliders and neutrino factories», *Rev. Accel. Sci. Technol.* **10**, 189 (2019).

- [64] J.P. Delahaye *et al.*, «Muon colliders», [arXiv:1901.06150](#) [physics.acc-ph].
- [65] N. Bartosik *et al.*, «Muon collider: the Low EMittance Muon Accelerator (LEMMA) approach», *PoS (LeptonPhoton2019)*, 047 (2019).
- [66] MICE Collaboration, «Demonstration of cooling by the Muon Ionization Cooling Experiment», *Nature* **578**, 53 (2020).
- [67] R.D. Ryne, «Muon colliders come a step closer», *Nature* **578**, 44 (2020).
- [68] N. Amapane *et al.*, «LEMMA approach for the production of low-emittance muon beams», *Nuovo Cim. C* **42**, 259 (2020).
- [69] K.R. Long *et al.*, «Muon colliders to expand frontiers of particle physics», *Nature Phys.* **17**, 289 (2021).
- [70] K. Cheung, Z.S. Wang, «Physical potential of a muon–proton collider», *Phys. Rev. D* **103**, 116009 (2021).
- [71] Y.C. Acar, U. Kaya, B.B. Oner, «Resonant production of color octet muons at Future Circular Collider-based muon–proton colliders», *Chinese Phys. C* **42**, 083108 (2018).
- [72] Y. Acar *et al.*, «Future circular collider based lepton–hadron and photon–hadron colliders: Luminosity and physics», *Nucl. Instrum. Methods Phys. Res. A* **871**, 47 (2017).
- [73] A. Caliskan, S.O. Kara, A. Ozansoy, «Excited muon searches at the FCC-based muon–hadron colliders», *Adv. High Energy Phys.* **2017**, 1540243 (2017).
- [74] M. Takeuchi, Y. Uesaka, M. Yamanaka, «Higgs mediated CLFV processes  $\mu N(eN) \rightarrow \tau X$  via gluon operators», *Phys. Lett. B* **772**, 279 (2017).
- [75] Y.C. Acar, U. Kaya, B.B. Oner, «Resonant production of color octet muons at Future Circular Collider-based muon–proton colliders», *Chinese Phys. C* **42**, 083108 (2018).
- [76] E. Alici, M. Köksal, «Probing the anomalous  $tq\gamma$  couplings through single top production at the future lepton–hadron colliders», *Mod. Phys. Lett. A* **34**, 1950298 (2019).
- [77] A. Ozansoy, «Investigating Doubly Charged Leptons at Future Energy Frontier Muon–Proton Colliders», *Communications Faculty of Sciences University of Ankara Series A2–A3: Physical Sciences and Engineering* **61**, 111 (2019).
- [78] S. Spor, A.A. Billur, M. Köksal, «Model independent study for the anomalous  $W^+W^-\gamma$  couplings at the future lepton–hadron colliders», *Eur. Phys. J. Plus* **135**, 683 (2020).
- [79] A. Belyaev, N.D. Christensen, A. Pukhov, «CalcHEP 3.4 for collider physics within and beyond the Standard Model», *Comput. Phys. Commun.* **184**, 1729 (2013).

- [80] A.V. Semenov, «LanHEP: a package for automatic generation of Feynman rules in field theory. Version 2.0», [arXiv:hep-ph/0208011](https://arxiv.org/abs/hep-ph/0208011).
- [81] A. Semenov, «LanHEP — A package for automatic generation of Feynman rules from the Lagrangian. Version 3.2», *Comput. Phys. Commun.* **201**, 167 (2016).
- [82] N. Bartosik *et al.*, «Detector and Physics Performance at a Muon Collider», *J. Instrum.* **15**, P05001 (2020).
- [83] M. Lu *et al.*, «The Physics Case for an Electron–Muon Collider», *Adv. High Energy Phys.* **2021**, 6693618 (2021).
- [84] F. Collamati *et al.*, «Advanced assessment of beam-induced background at a muon collider», *J. Instrum.* **16**, P11009 (2021).
- [85] P. Agostini *et al.*, «The large hadron–electron collider at the HL-LHC», *J. Phys. G: Nucl. Part. Phys.* **48**, 110501 (2021).
- [86] H.-L. Lai *et al.*, «New parton distributions for collider physics», *Phys. Rev. D* **82**, 074024 (2010).
- [87] H. Abramowicz *et al.*, «A Luminosity Calorimeter for CLIC», CERN Report LCD-Note-2009-002, 2009.
- [88] M. Cepeda *et al.*, «Report from Working Group 2: Higgs Physics at the HL-LHC and HE-LHC», *CERN Yellow Rep. Monogr.* **7**, 221 (2019).
- [89] L. Apanasevich *et al.*, «Sensitivity of Potential Future  $pp$  Colliders to Quark Compositeness», in: «Proceedings of the Community Summer Study on the Future of U.S. Particle Physics: Snowmass on the Mississippi», Minneapolis, MN, USA July 29–August 6, 2013.
- [90] R. Brun, F. Rademakers, «ROOT — An object oriented data analysis framework», *Nucl. Instrum. Methods Phys. Res. A* **389**, 81 (1997).